JACS
JOURNAL OF THE AMERICAN CHEMICAL SOCIETY

Article

A Revised Mechanism for the Kinugasa Reaction

Thomas C Malig, Diana Yu, and Jason E Hein

J. Am. Chem. Soc., **Just Accepted Manuscript** • DOI: 10.1021/jacs.8b04635 • Publication Date (Web): 02 Jul 2018

ACS Publications

is published by the American Chemical Society. 1155 Sixteenth Street N.W., Washington, DC 20036

A Revised Mechanism for the Kinugasa Reaction

Thomas C. Malig, Diana Yu, and Jason E. Hein*

Department of Chemistry, The University of British Columbia, Vancouver, BC V6T 1Z1, Canada

ABSTRACT: Detailed kinetic analysis for the Cu(I)-catalyzed Kinugasa reaction forming *β*-lactams has revealed an anomalous overall zero-order reaction profile, due to opposing positive and negative orders in nitrone and alkyne respectively. Furthermore, the reaction displays a second-order dependence on catalyst, confirming the critical involvement of a postulated bis-Cu complex. Finally, reaction progress analysis of multiple byproducts has allowed a new mechanism, involving a common ketene intermediate to be delineated. Our results demonstrate that *β*-lactam synthesis through the Kinugasa reaction proceeds via a cascade involving (3+2) cycloaddition, (3+2) cycloreversion and finally (2+2) cycloaddition. Our new mechanistic understanding has resulted in optimized reaction conditions to dramatically improve the yield of the target *β*-lactams and provides the first consistent mechanistic model to account for the formation of all common byproducts of the Kinugasa reaction.

INTRODUCTION

β-lactams represent a privileged scaffold in organic synthesis in addition to their important role as the core motif in *β*-lactam antibiotics such as penicillins, cephalosporins, monobactams, and carbapanems.[1,2] More recently molecules containing a *β*-lactam subunit have demonstrated additional therapeutic effects by functioning as antifungal,[3] anticancer,[4,5] and antiviral agents.[5,6] Furthermore, *β*-lactams make valuable synthons as they are readily amenable to subsequent functionalization to yield other biologically relevant building blocks such as *β*-amino acids and amino alcohols.[7] High yielding convergent methods for the syntheses of *β*-lactams capable of imparting both enantio- and diastereoselectivity are therefore of great value.

One such method for the direct syntheses of *β*-lactams was discovered by Kinugasa and Hashimoto in 1972 when they reported that treatment of a copper acetylide with a nitrone afforded *β*-lactams (Scheme 1).[8]

Scheme 1. The Kinugasa reaction

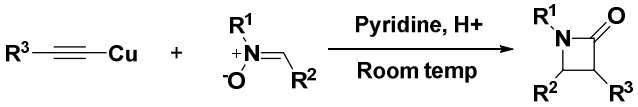

The Kinugasa reaction provides an attractive option for the syntheses of *β*-lactams because of its optimal atom economy, its employment of readily accessible starting materials, and due to the convergency of the approach. The utility of the Kinugasa reaction was increased when it was reported that corresponding *β*-lactams could be synthesized asymmetrically with *ee*'s up to 93%.[9] Despite the demonstrated usefulness of the reaction, there still exist several major limitations preventing it from being more universally adopted. A recent review article by Chmielewski in 2014 deemed the Kinugasa reaction "an "ugly duckling" of *β*-lactam chemistry".[10] The formation of multiple byproducts throughout the course of the reaction remains a significant obstacle, often resulting in modest yields of the desired *β*-lactams.

The mechanism of the Kinugasa reaction has been a topic of study for decades but remains an area of active research. Recently a working mechanism based on computational studies for the catalytic Kinugasa reaction was proposed (Scheme 2).[11] A key (3+2) cycloaddition between a copper acetylide (**5**) and nitrone (**2**) generates a transient cuprated heterocycle **6**.[11] It has been proposed that protonation of **7** at the nitrogen center facilitates *N-O* bond cleavage, forming an acyclic ketene intermediate **8**. Intramolecular cyclization of **8** yields a copper coordinated enolate **9**. Ligand exchange of copper, as well as a proton transfer affords a mixture of *β*-lactam diastereomers (**3**).

Scheme 2. Kinugasa reaction mechanism by Himo et al[11]

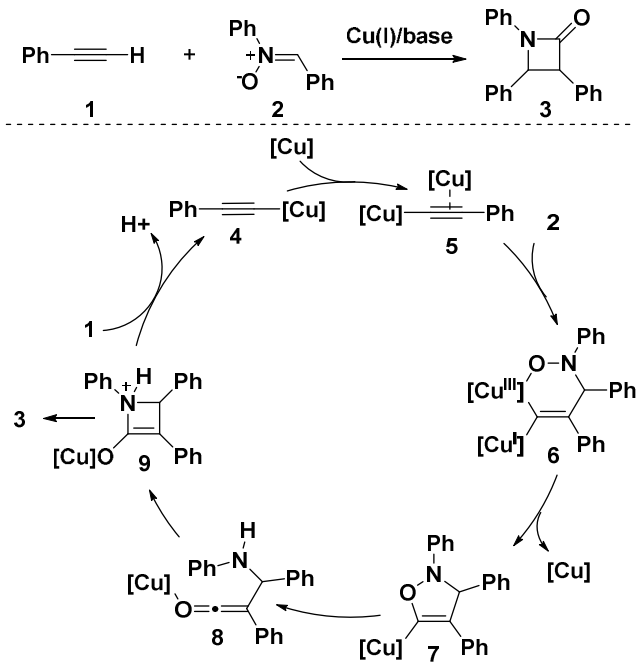

Despite the current understanding and synthetic usefulness of the Kinugasa reaction, to the best of our knowledge there exists no detailed kinetic analysis for this reaction. Herein, we report the use of reaction progress kinetic analysis (RPKA)[12,13] in conjunction with VTNA[14,15] to help delineate the underlying mechanism with the goal to increase the yield of lactams and provide insight into the pathways that form the undesired byproducts often associated with the reaction.

Reactions were monitored using a prototype robotic sampling apparatus coupled to HPLC-MS.[16] This device provides real-time quantitative reaction progress data, without the need for collection and quenching of aliquots, which would then be analyzed off-line following reaction completion.

Results and Discussion

Critical Importance of the Base Additive

Our investigation began by selecting a model reaction, utilizing tetrakis(acetonitrile)copper(I) tetrafluoroborate as the Cu(I) source, tris((1-cyclopentyl-1H-1,2,3-triazol-4-yl)methyl)amine (TCPTA) as the ligand, and diisopropylamine (DIPA) as the base. This choice of base was based on previous reports, where sterically encumbered secondary amines were found to give superior yields of the desired *β*-lactam.[17,18]

The reaction profile shows the formation of both *cis* and *trans* *β*-lactams (**3a** and **3b**, respectively), with the *cis* diastereomer being favoured (Figure 1). Unfortunately, the desired *β*-lactams were not the major product under these conditions, with *ca.* 60% of the initial starting materials being converted into the corresponding imine (**10**) and amide (**11**).

Imines are often reported as a major byproduct, with their formation has been attributed to Cu-catalyzed deoxygenation of the nitrone reagent.[19,20] Interestingly, **10** and **11** were consistently generated in a 1:1 ratio throughout the reaction. The observation of the uniform byproduct ratio is not consistent with the off-cycle deoxygenation hypothesis, and instead points to a common intermediate for generation of both lactam and imine/amide products.

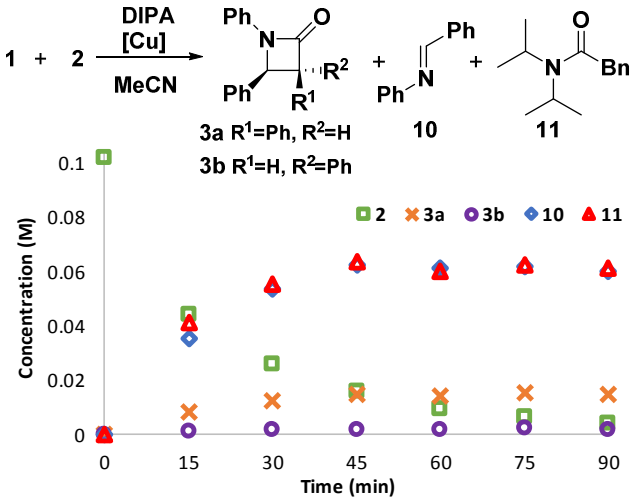

Figure 1. Reaction profile when DIPA was used as the basic additive. Reaction conditions: $[\mathbf{1}]_0 = [\mathbf{2}]_0 = [\text{DIPA}]_0 = 0.1$ M; $[Cu(MeCN)_4BF_4] = [\text{TCPTA}] = 0.01$ M.

The conserved 1:1 ratio between byproducts **10** and **11** likely stems from decomposition of the Cu-dihydroisoxazolide **7** intermediate (Scheme 3). This decomposition pathway would involve cleavage of **7** via a formal (3+2) retrocycloaddition, giving imine **10** and ketene **12**, the latter of which could be rapidly captured by a nucleophile (such as DIPA) to generate generic product **13**. Such a pathway is similar to the proposed rearrangement of *N*-sulfonyl Cu-triazolides **14**, which decompose to give the corresponding ketenimines (**15**) and nitrogen gas.[21] It should be noted that the formation of imine **10** and ketene **12** (by way of a Cu-ynoate intermediate) was originally proposed by Miura, who invoked a direct O-insertion between nitrone and Cu-acetylide.[19] However, our reaction progress and KIE measurements (vide infra) do not support this proposal.

Given this new mechanistic insight, unproductive formation of imine **10** and amide **11** may be arrested by using a stronger, non-nucleophilic amine base, such as DBU (1,8-diazabicyclo(5.4.0)undec-7-ene). This switch immediately led to an increased yield *β*-lactam (from 17% to 78%), with a concomitant reduction in imine **10** formation (Figure 2). It was also noted that DIPA and DBU conferred complementary diastereoselectivities of the *β*-lactam products. Using DBU the *trans* *β*-lactam (**3b**) was favoured in a ratio >4:1, while DIPA give the *cis* *β*-lactam (**3a**) preferentially. This change in diastereoselectivity has been reported by other researchers,[22] and has been attributed to epimerization from the *cis* lactam to the thermodynamically favoured *trans* geometry, made possible by the increased basicity of DBU. Using DBU eliminates the undesired amide **11**, however, the generation of imine **10** was not fully suppressed, and alkynyl imine **20** appears as a new byproduct (Scheme 4).

Scheme 3. Proposed retrocycloaddition of **7** and analogous reaction seen with N-sulfonyl-1,2,3-triazoles (**14**)

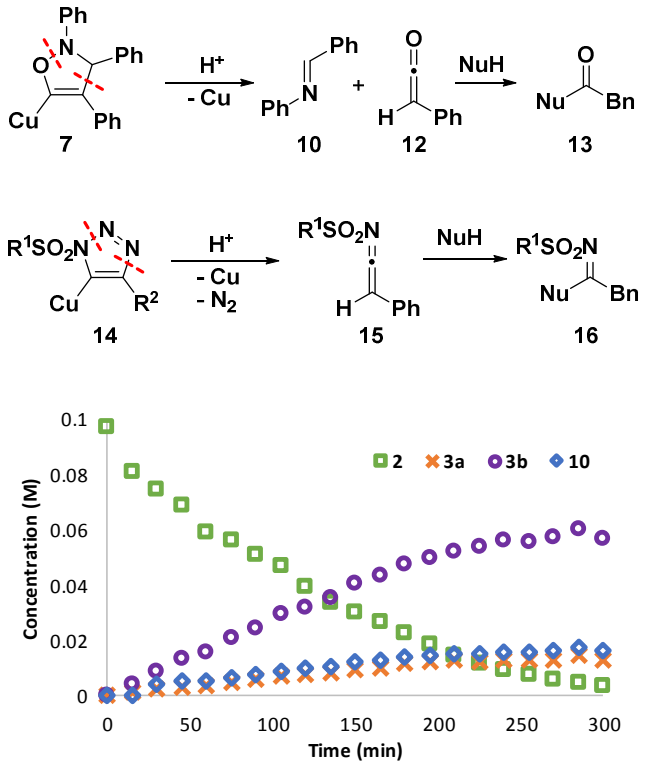

Figure 2. Reaction profile when DBU was used as the basic additive. Reaction conditions: $[\mathbf{1}]_0 = [\mathbf{2}]_0 = [\mathrm{DBU}]_0 = 0.1$ M, $[Cu(MeCN)_4BF_4] = [\mathrm{TCPTA}] = 0.01$ M.

Scheme 4. Proposed reaction pathway for the formation of imine **10** and alkynyl imine **20**.

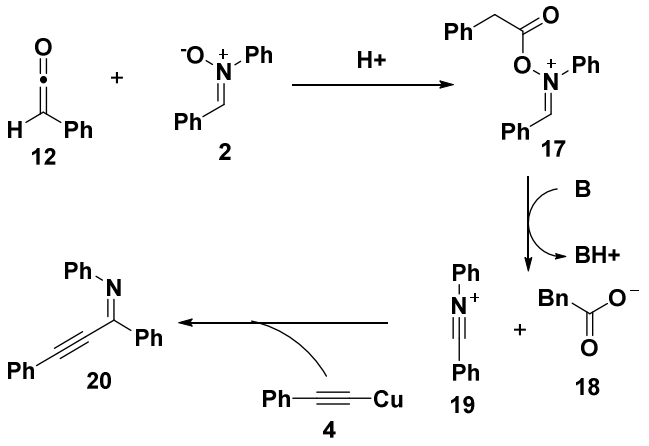

While, structurally unique from amide **11**, we believe the mechanism for its formation is closely related. In the absence of stronger nucleophiles, highly electrophilic ketene **12** is captured via the oxygen center of nitrone **2**. This acyl-nitrone (**17**) then fragments to give nitrilium **19** and 2-phenyl acetate (**18**), consistent with a proposal by Heine[23]. Finally, the highly electrophilic nitrilium is captured by copper acetylide **4** to afford alkynylimine **20**.

Kinetic Analysis to Identify Catalyst Resting State

To identify the catalyst resting state and test for any potential catalyst deactivation a series of same and different excess experiments were carried out.[12,13] Using the same excess protocol, there is a clear overlap in the kinetic profiles for the decay of [**2**] over time (Figure 3a) by applying a positive time shift to an experiment. This correlation confirms that neither product inhibition or catalyst deactivation is occurring under these conditions. Furthermore, this result contradicts proposals invoking direct Cu-catalyzed *N-O* deoxygenation of the nitrone to give either imine **10** or alkynylimine **20**. In these mechanisms, deoxygenation is coupled to the generation of Cu_2O. Thus, if this pathway was operative the catalyst activity would be modified as a function of reaction turnover as the speciation of the Cu-catalyst changes as it is converted to Cu_2O.

Next, a series of different excess experiments were conducted to probe the driving force in each reagent. While the overall reaction profile indicates the rate is nearly constant over time, varying the initial concentration of either alkyne **1** or nitrone **2** does have a substantial impact on the observed rate (Figure 3b). Specifically, increasing the initial concentration of **2** accelerates the reaction, indicting a positive order in [nitrone], while an increase in **1** leads to a decrease in rate consistent with a negative order in [alkyne]. These observed kinetic parameters suggest that interaction with **2** is involved the turnover limiting step, while **1** participates in an unproductive equilibrium, producing an off-cycle reservoir which modulates the concentration of available catalyst.

Finally, a series of experiments were carried out where the concentration of catalyst was varied from 5 – 20 mM (Figure 3c). This series confirms the system displays a positive order in catalyst, however initial inspection of the progress curves indicates that the response is greater than first order. Analyzing the reaction progress data for both varied initial substrate and catalysts (Figures 3b and c) using the variable time normalization analysis (VTNA) method allows the order in each component to be elucidated (see SI).[14,15] Under our reaction conditions the system obeys the rate law given in Equation 1.

(1) $Rate = k_{obs}[1]^{-1}[2]^{1}[cat]^{2}$

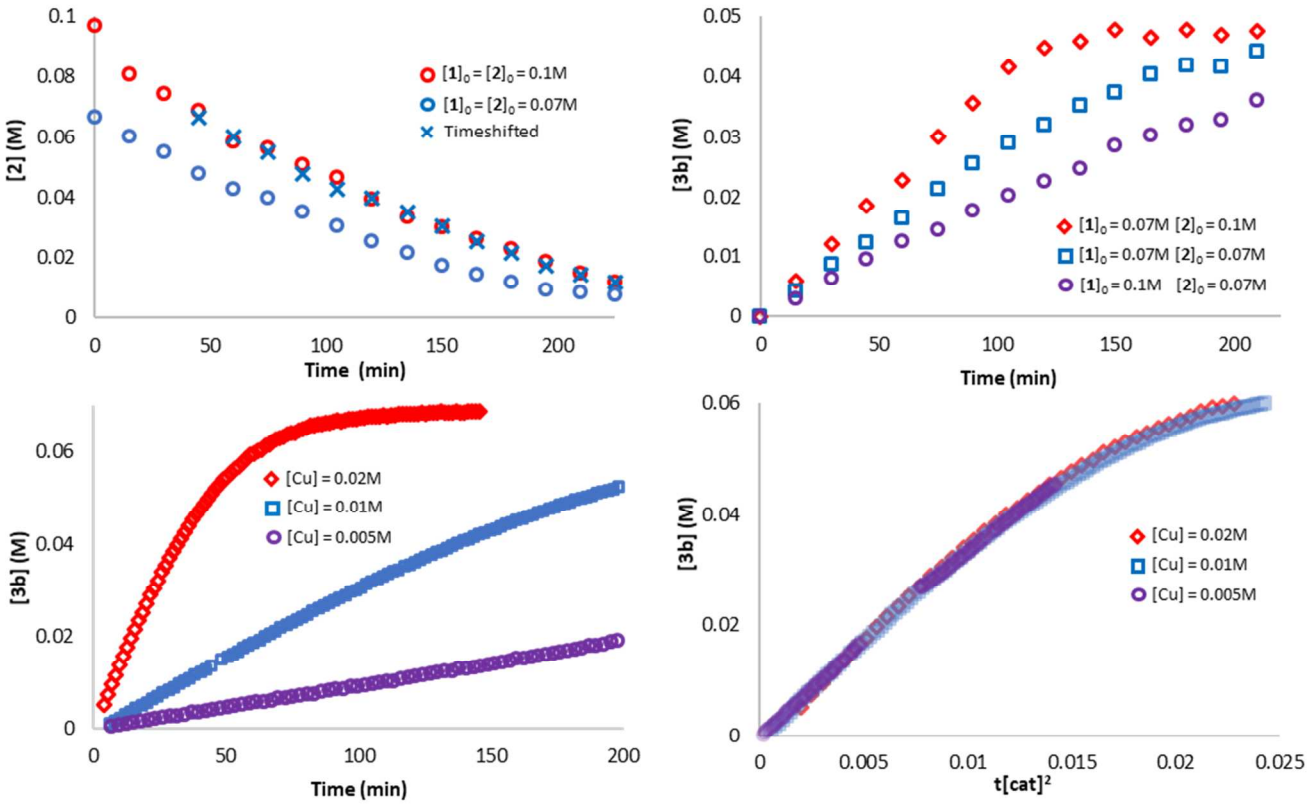

Figure 3. RPKA/VTNA Experiment Data (**a**) Same excess data for the reaction described in Figure 2 used to probe for catalyst deactivation and/or product inhibition. (**b**) Data from different excess experiments used to solve for order of **1** and **2.** (**c**) Kinetic data used of reactions outlined in Figure 2 but with various catalyst loadings, used to solve for catalyst order. (**d**) VTNA plot for data from Figure 3c indicating that the system is second order in [Cu].

These kinetic parameters allow key features of the mechanism to be elucidated. In particular, the second order dependence on the catalyst implies that two molecules of Cu are required in a kinetically important step of the catalytic cycle. This is consistent with the proposal by Himo, where cycloaddition between the nitrone and σ-Cu-acetylide was found to preferentially involve bis-Cu intermediate **5**.[11] Invoking bis-Cu complex **5** allows the cycloaddition to pass through 6-membered transition state **6**, which was predicted to be 4.6 kcal/mol lower in energy than the mono-Cu equivalent. Himo's calculation further predicted that the cycloaddition between bis-Cu complex **6** and nitrone **2** represented the highest energy barrier on the reaction coordinate, and thus is likely the turnover limiting step.

By adapting Himo's proposal it is possible to construct a simplified kinetic model to recapitulate the observed kinetic behaviors in the Kinugasa reaction (Scheme 5). First, the free $Cu(L)_x$ complex would bind to alkyne **1**, whereby deprotonation with DBU forms σ-Cu-acetylide **4**. Coordination of a second Cu(L)x species leads to π activation of the alkynyl system and gives bis-Cu complex **5**. Alternatively, capture of the σ-Cu-acetylide **4** with a second equivalent of alkyne would generate an off-cycle and unreactive polyacetylide aggregate (**4agg**). Productive catalysis would involve coordination of the nitrone to bis-Cu complex **5** followed by turnover-limiting cycloaddition via Himo's proposed 6-membered transition state produces a transient bis-Cu-intermediate, containing both a Cu(I) and Cu(III) center (**6**). Reductive elimination would liberate Cu-isoxazolide **7** and ultimately yield the *β*-lactams.

Scheme 5: Simplified mechanism representing the kinetically relevant steps in the overall pathway.

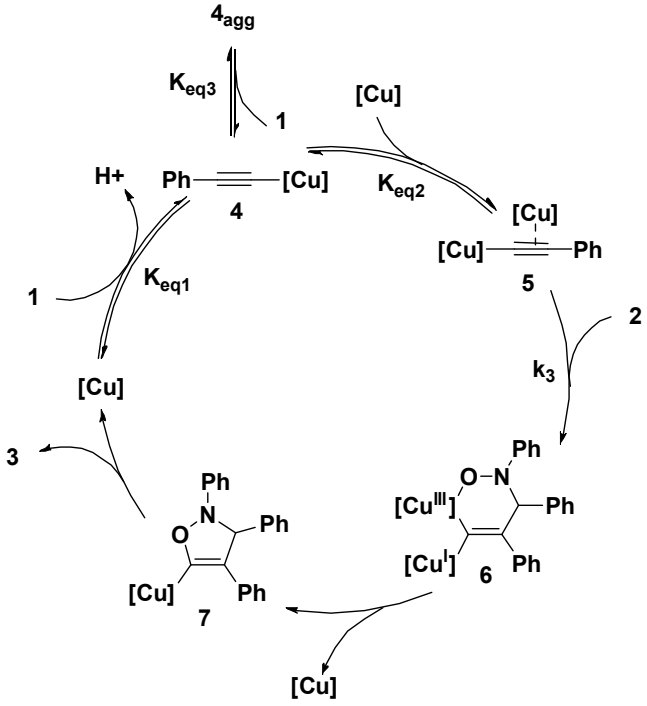

Deriving a steady state rate law for the proposed mechanism is possible by applying the quasi-equilibrium approximation for the three major processes involving the catalyst (K_{eq}^{1}, K_{eq}^{2} and K_{eq}^{3}). Using this approximation, expressions for each intermediate to be obtained as shown in Equations 2, 3 and 4.

$$(2)\quad K_{eq^1} = \frac{[\mathbf{4}]}{[Cu][\mathbf{1}]} \qquad [\mathbf{4}] = K_{eq^1}[Cu][\mathbf{1}]$$

$$(3)\quad K_{eq^2} = \frac{[\mathbf{5}]}{[Cu][\mathbf{4}]} \qquad [\mathbf{5}] = K_{eq^1}K_{eq^2}[Cu]^2[\mathbf{1}]$$

$$(4)\quad K_{eq^3} = \frac{[\mathbf{4}_{agg}]}{[\mathbf{4}][\mathbf{1}]} \qquad [\mathbf{1}]_{poly} = K_{eq^1}K_{eq^3}[Cu][\mathbf{1}]^2$$

Expressing the steady state rate law requires the free catalyst term [Cu] to be related to the total catalyst added via the mass balance equation (Equation 5). However, evaluating this equation is complicated as the complete form takes a quadratic form. However, the equilibrium between alkyne **1** and σ-Cu-acetylide **4** is anticipated to be strongly product favored due to the inclusion of 1 equivalent DBU, while the coordination of the second Cu will be comparatively much weaker. Thus, the catalyst mass balance equation can be simplified to the form shown in Equation 6.

$$(5)\quad [Cu]_{total} = K_{eq^1}K_{eq^2}[Cu]^2[\mathbf{1}] + [Cu](1 + K_{eq^1}[\mathbf{1}] + K_{eq^1}K_{eq^3}[\mathbf{1}]^2)$$

$$(6)\quad [Cu]_{total} \cong [Cu] + K_{eq^1}[Cu][\mathbf{1}] + K_{eq^1}K_{eq^3}[Cu][\mathbf{1}]^2$$

The first order relationship in [nitrone] indicates the cycloaddition between **5** and **2** represents the first irreversible step, and all subsequent rearrangements are not kinetically meaningful. Thus, the rate of reaction can be written with respect to this turnover limiting event (Equation 7) Solving for the unbound catalyst term [Cu] and substituting into the rate law gives the simplified rate law, Equation 8.

$$(7)\quad Rate = k_3[\mathbf{2}][\mathbf{5}] \cong k_3K_{eq^1}K_{eq^2}[\mathbf{1}][\mathbf{2}][Cu]^2$$

$$(8)\quad Rate \cong \frac{k_3K_{eq^1}K_{eq^2}[\mathbf{1}][\mathbf{2}][Cu]^2_{total}}{(1+K_{eq^1}[\mathbf{1}]+K_{eq^1}K_{eq^3}[\mathbf{1}]^2)^2}$$

The negative order relationship with respect to [alkyne] may reflect that, under strongly basic conditions of this reaction, the equilibrium between **1** and **4** is strongly product favored, while generation of the off-cycle polyacetylide complex involves a comparatively weaker interaction (K_{eq}^{1} >> 1 while K_{eq}^{3} << 1 respectively). By applying these assumption, the rate equation can be simplified to Equation 9, which reconciles the experimentally observed kinetic dependencies. It should be noted that the observation of an overall apparent zero-order reaction profile and second order in [Cu] is specific to the particular reagent concentrations from our study. Significant deviation from our simplified power law is expected when large excesses in either [alkyne] or [nitrone] are employed.

$$(9)\quad Rate \cong \frac{k_3K_{eq^2}[\mathbf{2}][Cu]^2_{total}}{K_{eq^1}[\mathbf{1}]}$$

Measurement of Competitive Secondary KIE

As kinetic studies (vide supra) suggest that numerous equilibrium binding events precede the turnover limiting coupling with nitrone **2**, a secondary interrogation of the key transition state was sought. By creating both H and D isotopologues of the nitrone, a series of kinetic isotope experiments (KIE) could be performed, monitoring both reaction rate and product selectivity using ^{1}H NMR. As the KIE experiments were to be performed utilizing NMR time-course analysis, the reaction behavior must match the HPLC analysis if the results were to be compared.[24] Performing the reaction in a static NMR tube produced a profile which is nearly identical to the HPLC trend (Figure 4), confirming that data acquisition using the on-line HPLC monitoring prototype accurately captures the reaction profile. Furthermore, the strong correlation between these two analytical methods validates the application of the NMR time course for KIE investigations.

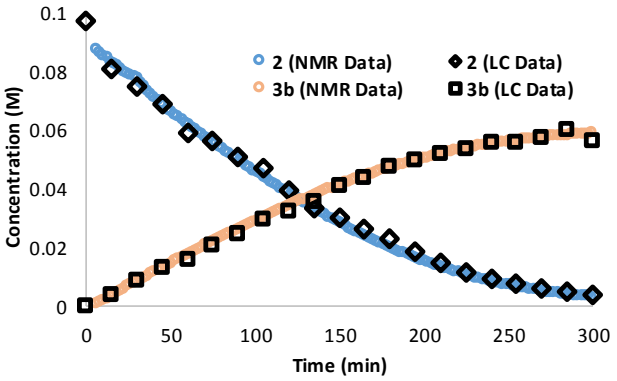

Figure 4. Comparison of reaction data gathered using HPLC prototype and by performing NMR time-course experiment in a static NMR tube. Reaction conditions are described in Figure 2.

A competition reaction was performed between proteo- and deutero- nitrones, **2** and **21** respectively, with alkyne **1**. The ^{1}H signals from the TCPTA ligand were clearly resolved and could be used as an internal standard, allowing the rate of change for each isotopologue of nitrone, *β*-lactam (both *cis* and *trans* diastereomers) and imine to be delineated. The ratio of nitrone isotopologues was plotted as a function of time, indicating that the rate of consumption of D-nitrone **21** is greater than the corresponding rate for H-nitrone **2** (Figure 5a)**.** Thus, the catalytic reaction exhibits an inverse secondary KIE under these reaction conditions.

To quantify the magnitude of the inverse KIE, another competition reaction was carried out, varying only the initial concentrations of H-and D-nitrone isotopologues. Assuming the reaction of both **2** and **21** obey the simplified rate law given in Equation 9, rates of reaction for each isotopologues will be modified both by [nitrone] but also the independent rate constants for the turnover limiting step associated with each isotopologue (k_3 in Scheme **7**). By manipulating Equation 9, the KIE for any experiment with varied initial concentrations of **2** and **21** can be expressed as Equation 10.

$$(10)\quad KIE = \frac{k_H}{k_D} = \frac{Rate_H[Nit_D]_\circ}{Rate_D[Nit_H]_\circ} = 0.95$$

The rate of consumption for each isotopologue follows a zero-order profile, and therefore is a constant given by the slope of

reaction profile (See SI for derivation). The reaction was found to display a secondary inverse KIE of 0.95, which suggests that the turnover limiting step involves a change in hybridization from sp^2 to sp^3 at the carbon bearing the isotopic label.[25] Applying the same analysis to our preliminary experiment with equimolar concentrations of both isotopologues (from Figure 5A) we observe an identical KIE of 0.95. These observations are consistent with the previous RPKA kinetic data, confirming that the initial (3+2) cycloaddition representing the turnover limiting step in the catalytic cycle.

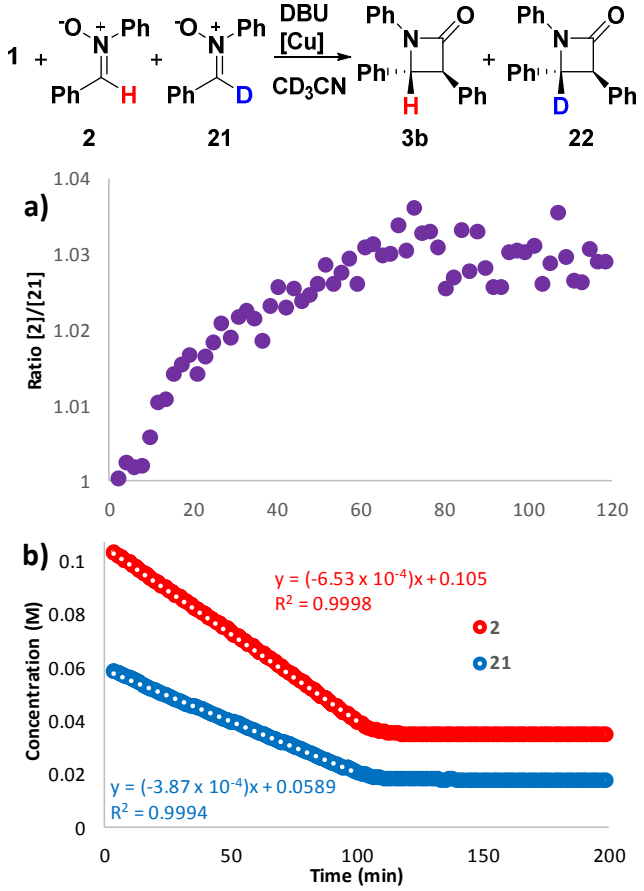

Figure 5. a) Variation in the ratio of nitrone isotopologues over the course of the KIE competition experiment. Reaction conditions: $[\mathbf{1}]_0 = [\mathbf{2}]_0 = [\mathbf{21}]_0 = [DBU]_0 = 0.1$ M. $[Cu(MeCN)_4BF_4] = [TCPTA] = 0.01$ M. **b)** Second KIE competition experiment used to solve for KIE from Equation 10. Reaction conditions: $[\mathbf{1}]_0 = [\mathbf{2}]_0 = [DBU]_0 = 0.1$ M, $[\mathbf{21}]_0 = 0.06$ M, $[Cu(MeCN)_4BF_4] = [TCPTA] = 0.01$ M.

Expanded Mechanistic Model

By combining our reaction progress and kinetic data, it is now possible to propose a complete mechanistic model that explains both the productive and unproductive reaction pathways (Scheme 6). First, the cycloaddition begins with the generation of the key σ-Cu(I) acetylide **4** from the terminal alkyne **1**. At high concentration of alkyne an off-cycle reservoir is created, restricting the Cu(I) available for productive cycloaddition and manifests as the negative order in [alkyne]. Further activation of the σ-Cu acetylide **4** by way of a second Cu(I) is required to effect cycloaddition and gives rise to the second order behavior in [Cu]. Coordination of the nitrone dipole and cycloaddition to produce metallocyclic intermediate **6** constitutes the turnover-limiting step, which is consistent with both the positive order in [nitrone] and inverse secondary KIE observed with isotopologue **21**.

From intermediate **6**, rapid reductive elimination followed by protonation and (3+2) cycloreversion gives ketene and imine (**12** and **10** respectively). The fate of these key intermediates governs the observed chemoselectivity of the reaction. If sufficiently nucleophilic reagents are present (such as DIPA or nitrone) capture of the highly electrophilic ketene dominates, diverting the reaction towards byproducts such as amide **11**, alkynylimine **20** and imine **10**. Alternatively, recombination of **10** and **12** via a Lewis acid catalyzed (2+2) cycloaddition yields the desired *β*-lactams. Under this revised mechanism, Cu(I)-catalyzed *β*-lactam generation between terminal alkynes and nitrones is better classified as a cascade reaction, terminating with a formal (2+2) cycloaddition, more classically known as the Staudinger synthesis of *β*-lactams.[26] This revised pathway is analogous to the formation of *N*-sulfonylazetidin-2-imines via capture of ketenimine **14** with imines.[21]

Scheme 6. Proposed reaction mechanism based on kinetic data highlighting all key equilibria and binding events

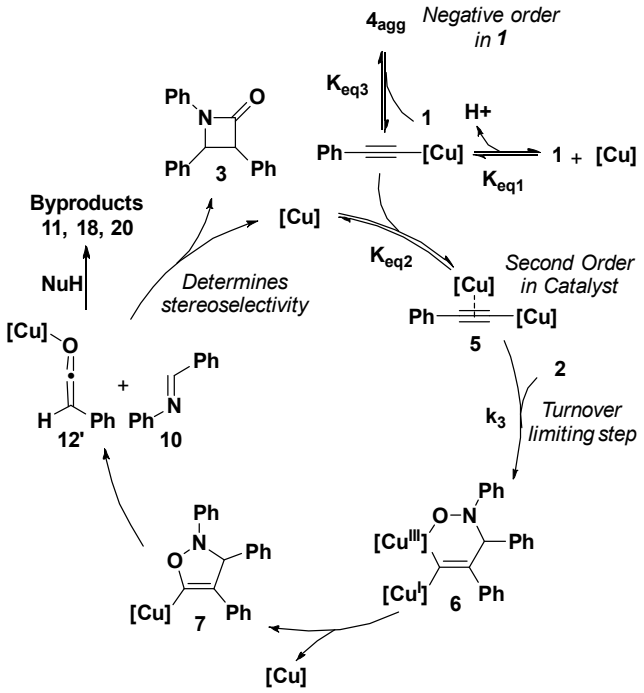

Our revised mechanism is not only consistent with the available kinetic data but also resolves two important inconsistencies with previous models. First, the intermediacy of the ketene **12** provides the first consistent model rationalizing both the formation of target *β*-lactams and common byproducts, including imine **10**, amide **11**, alkynylimine **20,** and benzyl carboxylate **18**. While similar byproducts have been documented, underlying mechanistic rationale for their appearance has been variable.[19] For example, Miura found that alkynylimines could be chemoselectively formed by using dppe (1,2-bis(diphenylphosphino)ethane). However, their proposed pathway required direct addition of the σ-Cu(I) acetylide to the nitrone sp^2 carbon, followed by deoxygenation to give Cu_2O. Our RPKA data is not consistent with Miura's proposal, as there is no evidence of catalyst deactivation or change in catalyst activity (Figure 3a) which would be apparent if $CuBF_4$ was being transformed to Cu_2O during the reaction.

A second important consequence of our modified mechanism relates to the stereocontrolling step. The geometry of the asymmetric center in the *β*-lactam is set by the (2+2) cycloaddition between ketene **12** and imine **10**, not the initial (3+2) cycloaddition involving the nitrone and σ-Cu(I) acetylide as is conventionally proposed. Thus, ligands, such as PyBOX, generate a Cu(I) complex that acts as a chiral Lewis acid to give stereodiscrimination akin to an asymmetric Staudinger synthesis. This modification resolves an issue noted by Himo, who found that incorporating chiral ligands onto the key bis-Cu-intermediate **5** creates numerous steric penalties, raising the energy of the chiral transition state above that of the uncatalyzed thermal (3+2) Huisgen dipolar cycloaddition.

One final consideration relates to the work by Shintani and Fu, who designed conditions to trap the proposed Cu-enolate, which would be formed after intramolecular cyclization of intermediate **8**.[27] This result is still consistent in the context of our modified mechanism, as both Fu's conditions and ours operate under stoichiometric strong base additives. Thus, it is possible that the allylation occurs after the formation of the *β*-lactam via base promoted enolate formation.

Confirmation of the Intermediacy of Ketene

To assess the participation of a Staudinger-like (2+2) coupling in the formation of the *β*-lactam products, a cross-over experiment was conducted. The reaction of **1** and **2** was performed in the presence of imine **23**, giving both the expected lactam **3b** as well as the newly observed cross-over product lactam **24** (Scheme 7). Control experiments have been conducted confirming that oxygen exchange between imine **23** and nitrone **2** does not appear to be occurring on the timescale of the cycloaddition (see supporting information for details). This result suggests that an exogenously dosed imine can participate in a formal (2+2) cycloaddition and provides additional evidence that ketene **12** is an intermediate in the productive lactam-forming pathway. The relatively low concentration of the cross-over product **24** further suggests that if a formal (2+2) reaction is ultimately responsible for the generation of the *β*-lactam, that it proceeds via an inner sphere mechanism involving rapid coupling between **12'** and **10**, which does not allow facile exchange of the exogenous imine coupling partner. Similar lack of positive cross-over results have been reported in Tsuji-Trost like processes where molecular fragments remain tightly bound prior to recapture.[28] This proposal is further supported by our kinetic evidence, which suggests that the cycloreversion and subsequent recapture are rapid relative to the initial (3+2) coupling between nitrone and Cu-acetylide.

Scheme 7. Crossover experiment designed to probe for intermediacy of ketene **12**. Ar = *p*-tolyl. $[\mathbf{1}]_0 = [\mathbf{2}]_0 = [\mathrm{DBU}]_0 = 0.1$ M, $[\mathbf{23}]_0 = 0.025$ M, [CuI] = [TCPTA] = 0.01 M.

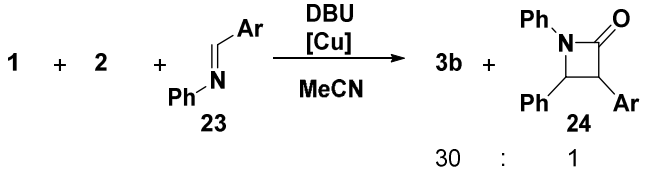

CONCLUSIONS

To summarize, we have reported the use of RPKA to delineate the underlying mechanism of the Kinugasa reaction. These experiments reveal that the system displays an overall zero-order profile, brought about by a near integer order of +1 and -1 for [nitrone] and [alkyne] respectively. Furthermore, the kinetic data reveal that an initial (3+2) cycloaddition between doubly activated bis-Cu(I) acetylide and nitrone constitutes the turnover limiting step. This conclusion is supported by the second order behavior with respect to [Cu] as well as a secondary inverse kinetic isotope effect of 0.95 for deuterated nitrone isotopologues. The observed kinetic and chemoselectivity data allow us to propose a modified mechanism, involving a novel (3+2) cycloreversion followed by Lewis acid catalyzed (2+2) cycloaddition. Most importantly, our new catalytic pathway, which proceeds via a common ketene intermediate, provides the first consistent mechanistic model for the generation of all commonly observed byproducts of the Kinugasa reaction. By understanding the pivotal role of the cycloaddition reaction cascade and the intermediacy of the reactive ketene we have been able to derive reaction conditions using non-nucleophilic bases (such as DBU), which improves the yield of the desired *β*-lactam products to ~80%.

ASSOCIATED CONTENT

Supporting Information

The Supporting Information is available free of charge on the ACS Publications website.
Experimental procedures and characterization data

AUTHOR INFORMATION

Corresponding Author

* jhein@chem.ubc.ca

ORCID

Jason E. Hein: 0000-0002-4345-3005

ACKNOWLEDGMENT

The authors gratefully acknowledge Prof. Paul Cheong for helpful discussion and insight into experimental design. In addition, we acknowledge Mettler-Toledo Autochem for generous donation of process analytical equipment (EasyMax). Financial support for this work was provided by the University of British Columbia and the Natural Sciences and Engineering Resource Council of Canada for both research (2016-RGPIN-04613) and student support (NSERC-CGS to T. C. M.).

REFERENCES

(1) Galletti, P.; Giacomini, D. Monocyclic β-Lactams: New Structures for New Biological Activities. *Curr. Med. Chem.* **2011**, *18*, 4265–4283.

(2) Singh, G. S. β-Lactams in the New Millennium. Part-I: Monobactams and Carbapenems. *Mini-Reviews Med. Chem.* **2004**, *4*, 69–92.

(3) Keri, R. S.; Hosamani, K. M.; Reddy, H. S.; Shingalapur, R. V. Synthesis, in-Vitro Antimicrobial and Cytotoxic Studies of Novel Azetidinone Derivatives. *Arch. Pharm.* **2010**, *343*, 237–247.

(4) Indrani Banik; Frederick F. Becker, A.; Banik, B. K.

Stereoselective Synthesis of β-Lactams with Polyaromatic Imines: Entry to New and Novel Anticancer Agents. *J. Med. Chem* **2002**, *46*, 12–15.

(5) Bonneau, P. R.; Hasani, F.; Plouffe, C.; Malenfant, E.; LaPlante, S. R.; Guse, I.; Ogilvie, W. W.; Plante, R.; Davidson, W. C.; Hopkins, J. L.; Morelock, M. M.; Cordingley, M. G; Deziel, R.. Inhibition of Human Cytomegalovirus Protease by Monocyclic β-Lactam Derivatives: Kinetic Characterization Using a Fluorescent Probe. *J. Am. Chem. Soc.* **1999**, *121*, 2965–2973.

(6) Gerona-Navarro, G.; Pérez De Vega, M. J.; García-López, M. T.; Andrei, G.; Snoeck, R.; De Clercq, E.; Balzarini, J.; González-Muñiz, R. From 1-Acyl-β-Lactam Human Cytomegalovirus Protease Inhibitors to 1-Benzyloxycarbonylazetidines with Improved Antiviral Activity. A Straightforward Approach to Convert Covalent to Noncovalent Inhibitors. *J. Med. Chem.* **2005**, *48*, 2612–2621.

(7) Ojima, I.; Delaloge, F. Asymmetric Synthesis of Building-Blocks for Peptides and Peptidomimetics by Means of the β-Lactam Synthon Method. *Chem. Soc. Rev.* **1997**, *26*, 377–386.

(8) Kinugasa, M.; Hashimoto, S. The Reactions of copper(I) Phenylacetylide with Nitrones. *J. Chem. Soc. Chem. Commun.* **1972**, *0*, 466.

(9) Lo, M. M.-C.; Fu, G. C. Cu(I)/Bis(azaferrocene)-Catalyzed Enantioselective Synthesis of β-Lactams via Couplings of Alkynes with Nitrones. *J. Am. Chem. Soc.* **2002**, *124*, 4572–4573.

(10) Stecko, S.; Furman, B.; Chmielewski, M. Kinugasa Reaction: An "ugly Duckling" of β-Lactam Chemistry. *Tetrahedron* **2014**, *70*, 7817–7844.

(11) Santoro, S.; Liao, R.-Z.; Marcelli, T.; Hammar, P.; Himo, F. Theoretical Study of Mechanism and Stereoselectivity of Catalytic Kinugasa Reaction. *J. Org. Chem.* **2015**, *80*, 2649–2660.

(12) Blackmond, D. G. Reaction Progress Kinetic Analysis: A Powerful Methodology for Mechanistic Studies of Complex Catalytic Reactions. *Angew. Chem. Int. Ed.* **2005**, *44*, 4302–4320.

(13) Blackmond, D. G. Kinetic Profiling of Catalytic Organic Reactions as a Mechanistic Tool. *J. Am. Chem. Soc.* **2015**, *137*, 10852–10866.

(14) Burés, J. Variable Time Normalization Analysis: General Graphical Elucidation of Reaction Orders from Concentration Profiles. *Angew. Chem. Int. Ed.* **2016**, *55*, 16084–16087.

(15) Burés, J. A Simple Graphical Method to Determine the Order in Catalyst. *Angew. Chem. Int. Ed.* **2016**, *55*, 2028–2031.

(16) Malig, T. C.; Koenig, J. D. B.; Situ, H.; Chehal, N. K.; Hultin, P. G.; Hein, J. E. Real-Time HPLC-MS Reaction Progress Monitoring Using an Automated Analytical Platform. *React. Chem. Eng.* **2017**, *2*, 309–314.

(17) Ye, M. C.; Zhou, J.; Tang, Y. Trisoxazoline/Cu(II)-Promoted Kinugasa Reaction. Enantioselective Synthesis of β-Lactams. *J. Org. Chem.* **2006**, *71*, 3576–3582.

(18) Ye, M.-C.; Zhou, J.; Huang, Z.-Z.; Tang, Y. Chiral tris(oxazoline)/Cu(II) Catalyzed Coupling of Terminal Alkynes and Nitrones. *Chem. Commun.* **2003**, *0*, 2554.

(19) Miura, M.; Enna, M.; Okuro, K.; Nomura, M. Copper-Catalyzed Reaction of Terminal Alkynes with Nitrones. Selective Synthesis of 1-Aza-1-Buten-3-Yne and 2-Azetidinone Derivatives. *J. Org. Chem.* **1995**, *60*, 4999–5004.

(20) Mames, A.; Stecko, S.; Mikołajczyk, P.; Soluch, M.; Furman, B.; Chmielewski, M. Direct, Catalytic Synthesis of Carbapenams via Cycloaddition/Rearrangement Cascade Reaction: Unexpected Acetylenes' Structure Effect. *J. Org. Chem.* **2010**, *75*, 7580–7587.

(21) Whiting, M.; Fokin, V. V. Copper-Catalyzed Reaction Cascade: Direct Conversion of Alkynes intoN-Sulfonylazetidin-2-Imines. *Angew. Chem. Int. Ed.* **2006**, *45*, 3157–3161.

(22) Zhang, X.; Hsung, R. P.; Li, H.; Zhang, Y.; Johnson, W. L.; Figueroa, R. A Highly Stereoselective Synthesis of Chiral α-Amino-β-Lactams via the Kinugasa Reaction Employing Ynamides. *Org. Lett.* **2008**, *10*, 3477–3479.

(23) Heine, H. W.; Zibuck, R.; VandenHeuvel, W. J. A. Mechanisms for the Reactions of Nitrones with Aroyl Chlorides. *J. Am. Chem. Soc.* **1982**, *104*, 3691–3694.

(24) Foley, D. A.; Dunn, A. L.; Zell, M. T. Reaction Monitoring Using Online vs Tube NMR Spectroscopy: Seriously Different Results. *Magn. Reson. Chem.* **2016**, *54*, 451–456.

(25) Anslyn, E. V.; Dougherty, D. A. *Modern Physical Organic Chemistry*; University Science, 2006.

(26) Staudinger, H. Zur Kenntniss Der Ketene. Diphenylketen. *Justus Liebig's Ann. der Chemie* **1907**, *356*, 51–123.

(27) Shintani, R.; Fu, G. C. Catalytic Enantioselective Synthesis Ofβ-Lactams: Intramolecular Kinugasa Reactions and Interception of an Intermediate in the Reaction Cascade. *Angew. Chem. Int. Ed.* **2003**, *42*, 4082–4085.

(28) Al-Amin, M.; Roth, K. E.; Blum, S. A. Mechanistic Studies of Gold and Palladium Cooperative Dual-Catalytic Cross-Coupling Systems. *ACS Catal.* **2014**, *4*, 622–629.

.

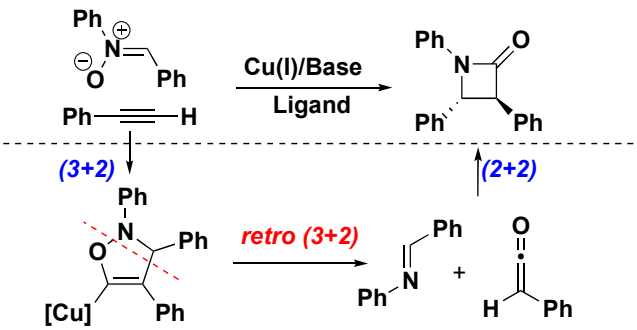
Ph
N
O
Ph
Ph
H
Cu(I)/Base
Ligand
Ph
N
O
Ph
Ph
(3+2)
(2+2)
Ph
N
O
Ph
[Cu]
Ph
retro (3+2)
Ph
N
Ph
+
O
H
Ph